



11-15-2007

## Searching for the Source: Determining $\text{NAD}^+$ Concentrations in the Yeast Vacuole

Camille Hardiman  
*University of Pennsylvania*

---

# Searching for the Source: Determining NAD<sup>+</sup> Concentrations in the Yeast Vacuole

## Abstract

The burgeoning field of bioremediation relies on the natural abilities of plants and fungi to accumulate certain toxic heavy metals. In heavy metal detoxification, plant and yeast vacuoles are responsible for the sequestration of toxins away from the cytoplasm. A yet-unpublished study done by the Rea group analyzed the protein profile of the vacuolar lumen in the budding yeast *Saccharomyces cerevisiae*. Several NAD<sup>+</sup>-dependent dehydrogenases were found within this compartment, a surprising finding in light of the yeast vacuole's predominantly lytic function. Five of these enzymes were found to increase in level in the vacuole during heavy metal stress. Moreover, when vacuolar lysates were assayed *in vitro*, they were found to contain dehydrogenase activity when exogenous NAD<sup>+</sup> or NADH was provided. If these enzymes are also active in this compartment *in vivo*, the question is raised: from where do the cofactors required for the reactions that these enzymes catalyze come? If these enzymes had a vacuolar source of NAD<sup>+</sup>, they could also potentially be active *in vivo*. Thus, in the present project, we are seeking to determine the concentration of NAD<sup>+</sup> inside the vacuole of *S. cerevisiae*. Toward this end, high-purity "proteomics-grade" intact vacuoles were isolated from *S. cerevisiae* by a combination of differential, density, and floatation centrifugation. NAD<sup>+</sup> was then extracted by acid precipitation and solvent extraction to separate vacuolar proteins from cofactor. NAD<sup>+</sup> was quantified using a two-step redox-coupled reaction system containing phenazine methosulfate (PMS) as mediator and thiazoyl blue tetrazolium bromide (MTT) as terminal electron acceptor. The spectrophotometric measurement of reduced MTT at 570 nm is an indirect measure of the initial NAD<sup>+</sup> concentration. To provide a basis for comparison, the estimated NAD<sup>+</sup> content of isolated vacuoles was compared to that of spheroplasts lysates extracted and assayed identically. The results indicate that the intravacuolar concentration of NAD<sup>+</sup> is two orders of magnitude lower than that of the spheroplast (5.2 vs. 202 μM), which may have implications for this redox-active cofactor's function in the vacuole. These findings may necessitate the reconsideration of the role played by vacuolar dehydrogenases in yeast cell metabolism (and possibly the metabolism of other vacuolate cells). Our findings suggest that the vacuolar pool of NAD<sup>+</sup> may be sufficient for utilization in the vacuole.

## Keywords

yeast vacuole, NAD, dehydrogenases, storage and salvage

## Cover Page Footnote

This work was supported by the Department of Biology at the University of Pennsylvania, and the Ronald E. McNair Post Baccalaureate Scholars Program. I thank Dr. Jean-Emmanuel Sarry, Richard Collum, and Dr. Philip A. Rea for their contributions to this work.

# Searching for the Source: Determining NAD<sup>+</sup> Concentrations in the Yeast Vacuole

Camille Hardiman, Jean-Emmanuel Sarry, and Philip A. Rea  
Plant Science Institute, Department of Biology  
University of Pennsylvania, Philadelphia, PA 19104

## Abstract

The burgeoning field of bioremediation relies on the natural abilities of plants and fungi to accumulate certain toxic heavy metals. In heavy metal detoxification, plant and yeast vacuoles are responsible for the sequestration of toxins away from the cytoplasm. A yet-unpublished study done by the Rea group analyzed the protein profile of the vacuolar lumen in the budding yeast *Saccharomyces cerevisiae*. Several NAD<sup>+</sup>-dependent dehydrogenases were found within this compartment, a surprising finding in light of the yeast vacuole's predominantly lytic function. Five of these enzymes were found to increase in level in the vacuole during heavy metal stress. Moreover, when vacuolar lysates were assayed *in vitro*, they were found to contain dehydrogenase activity when exogenous NAD<sup>+</sup> or NADH was provided. If these enzymes are also active in this compartment *in vivo*, the question is raised: from where do the cofactors required for the reactions that these enzymes catalyze come? If these enzymes had a vacuolar source of NAD<sup>+</sup>, they could also potentially be active *in vivo*. Thus, in the present project, we are seeking to determine the concentration of NAD<sup>+</sup> inside the vacuole of *S. cerevisiae*. Toward this end, high-purity "proteomics-grade" intact vacuoles were isolated from *S. cerevisiae* by a combination of differential, density, and floatation centrifugation. NAD<sup>+</sup> was then extracted by acid precipitation and solvent extraction to separate vacuolar proteins from cofactor. NAD<sup>+</sup> was quantified using a two-step redox-coupled reaction system containing phenazine methosulfate (PMS) as mediator and thiazoyl blue tetrazolium bromide (MTT) as terminal electron acceptor. The spectrophotometric measurement of reduced MTT at 570 nm is an indirect measure of the initial NAD<sup>+</sup> concentration. To provide a basis for comparison, the estimated NAD<sup>+</sup> content of isolated vacuoles was compared to that of spheroplasts lysates extracted and assayed identically. The results indicate that the intravacuolar concentration of NAD<sup>+</sup> is two orders of magnitude lower than that of the spheroplast (5.2 vs. 202 μM), which may have implications for this redox-active cofactor's function in the vacuole. These findings may necessitate the reconsideration of the role played by vacuolar dehydrogenases in yeast cell metabolism (and possibly the metabolism of other vacuolate cells). Our findings suggest that the vacuolar pool of NAD<sup>+</sup> may be sufficient for utilization in the vacuole.

**Keywords:** yeast vacuole, NAD, dehydrogenases, storage and salvage.

## Introduction

Contamination of soil and water by toxic heavy metals represents a major environmental hazard to human health. Among these pollutants, cadmium is a widespread, non-essential heavy metal released into the environment by human activities including agriculture, mining, and industry. The anthropogenic emission of cadmium, classified as a human carcinogen, is estimated at 29,190 tons per year.<sup>1</sup> Cadmium and nickel are among the metals that plant systems can hyperaccumulate and remove from contaminated sites. In heavy metal detoxification, plant and yeast vacuoles sequester metals like cadmium away from the cytoplasm.<sup>2</sup> The vacuole is the largest cellular organelle, taking up 20-90% of the total cell volume. It is responsible for storage, metabolite recycling, macromolecule breakdown, and ion homeostasis, in addition to toxin (e.g., heavy metal) detoxification. Thus, it is a critical site in understanding the biochemical pathways of a plant's response to metal poisoning, with potential implications in refining phytoremediation techniques.

A recent proteomics platform of the yeast vacuole was performed by Sarry et al. (2006),<sup>3</sup> where not only resident lytic vacuolar proteins but also several dehydrogenases were found to be catalytically competent (see Figure 1). Since these dehydrogenases, found active *in vitro*, are involved in oxidation reactions, they were not expected to be localized in the primarily lytic vacuole. The role of these enzymes in the vacuole is unknown, but represents an interesting line of inquiry, considering that one of these enzymes, alcohol dehydrogenase (ADH), may be involved in binding cadmium.<sup>4</sup> Further, all seven enzymes are dependent on nicotinamide adenine dinucleotide (NAD<sup>+</sup>) as their cofactor (see Table 1). NAD<sup>+</sup>, a derivative of niacin (vitamin B3), is a critical metabolic enzyme used as an oxidizing agent to reduce carbohydrate substrates. The mitochondria and cytoplasm are major sites of NAD<sup>+</sup> biosynthesis and storage, but little is known about the storage and subcellular distribution of NAD<sup>+</sup> in yeast. The possibility of NAD<sup>+</sup> localization inside of the vacuole is a critical path of investigation considering the localization of NAD<sup>+</sup>-dependent enzymes inside of the vacuolar lumen. A precedent for cofactor localization in vacuoles was recorded by the Hanson and Rea groups (2005),<sup>5</sup> where folate was unexpectedly found to be stored inside of vacuoles of red beet roots and pea leaves. Folate (vitamin B9) is a crucial cofactor in cerebral health, with defects possibly leading to dementia, atherosclerosis, and congestive heart failure.<sup>6,7</sup> The vacuoles were analyzed for their folate content, and were found to have a significant store, greater than that in the chloroplast, known as one of folate's storage sites.

Since little is published on cofactor localization inside of the vacuole, the discovery of folate inside of the vacuole may open up the possibility of other types of cofactors being stored there as well. And thus, if the five dehydrogenases that are active *in vitro* similarly had a vacuolar source of NAD<sup>+</sup>, they could potentially be active *in vivo* as well. There are several important implications of these enzymes being active *in vivo*, the foremost being insight into the larger function of the vacuole. Thus, in the present experiment, we are seeking to determine the concentration of NAD<sup>+</sup> in the *S. cerevisiae* vacuole.

## Experimental Procedures

*Yeast strains and growth conditions:* Wild-type *S. cerevisiae* strain DTY165 used in the present analysis was grown in YPD medium (10 g/L yeast extract, 20 g/L Bactopectone, dextrose 20 g/L; pH 5.5) at 30°C to an OD<sub>600nm</sub> between 1.5 and 2.0.

*Spheroplast isolation:* Using a procedure described in Sarry et al. (2006),<sup>3</sup> the cell wall was digested away from the yeast spheroplast (see Figure 2). Briefly, 500 mL of culture was grown overnight and centrifuged for 5 minutes at 4,000 rpm (Beckman J2-21 Centrifuge, JA-10 Rotor). It was then resuspended in 200 mL of deionized water, and centrifuged again for 5 minutes at 4 K. The pellet was then washed in 100 mL of first wash buffer (100 mM Tris-HCl, pH 9.4, and 10 mM DTT; all reagents acquired from Sigma). After a 20-minute incubation, samples were centrifuged again for 5 minutes at 4,000 rpm. The cell wall was digested by resuspending with digestion buffer (0.7 M sorbitol, 100 mM Tris-HCl, pH 7.5, 5.0 mM DTT, 50 mg Zymolase T-20; all reagents from Sigma) and incubating for 90 minutes at 30°C in a shaking water bath. Isolated spheroplasts were centrifuged again at 3,000 rpm at 4°C for minutes.

*Density gradient purification:* To obtain high-purity “proteomics-grade” intact vacuoles, isolated spheroplasts were loaded onto six ice-cold gradient tubes. The gradients consisted of three layers: sucrose/Ficoll Buffer filled the bottom layer, prepared with sucrose Buffer with 2.5% Ficoll (w/v). Preparing the next two layers involved first 4.0 mL of a 2:1, and 7.0 mL of a 3:1 ratio of sorbitol (0.6 M sorbitol, 10mM citrate-NaOH, pH 6.8 in 1.0 L) to sucrose (0.6 M Sucrose, 10 mM Citrate-NaOH, pH 6.8 in 500 mL) buffers. All gradient sections contained 10 L/mL solution of 1.0 M DTT and protease inhibitor cocktail (Sigma P8215, for fungal and yeast extracts). This mixture was centrifuged at 24,000 rpm for 1 hour (SW-28 Rotor, Beckman L7-55 Ultracentrifuge). Vacuoles were collected at the sucrose/Ficoll and 2:1 sorbitol:sucrose interface, washed in sorbitol buffer, and centrifuged at 3,000 rpm for 20 minutes.

*Vacuolar purity assessments:* Two assessments were performed to test the integrity and purity of the vacuolar extraction procedure. First, carboxypeptidase Y (CPY) and aminopeptidase I (APE1) are two vacuolar luminal markers, while  $\alpha$ -mannosidase is a vacuolar membrane marker (see Table 2). These luminal and membrane-bound enzymes both increased in activity and were co-purified, suggesting that vacuolar integrity was maintained: the membrane did not break and re-seal during the vacuole isolation procedure. Second, monochlorobimane (MCB) was also used as a test of the purity of the vacuole preparation (see Figure 3). MCB becomes fluorescent once it conjugates with glutathione (GSH) to yield a bimane-GS complex. Once it binds and is transported into the vacuole, its fluorescence is tracked and measured. This suggests that small molecules, like bimane-GS and  $\text{NAD}^+$ , are capable of being retained and measured inside of the vacuole despite the stress of the isolation procedure.

*$\text{NAD}^+$  extraction:* Isolated vacuoles and spheroplasts were each divided into two equivalent aliquots, centrifuged for 5 minutes at 10,000 rpm. After removal of the supernatant, the first aliquot was resuspended with 500  $\mu\text{L}$  Lysis Buffer (5 mM Tris-HCl, pH 7.5, 5 mM DTT, 10  $\mu\text{L}$  protease inhibitor cocktail in 10 mL) and put on ice for protein and enzyme assays. The second aliquot was resuspended with 300  $\mu\text{L}$  0.1M HCl, and then immediately neutralized with 150  $\mu\text{L}$  1.0M Tricine/KOH pH 9.3. The sample was incubated in a 100°C heat bath for 5 minutes, placed into an ice bucket for 5 minutes, and then centrifuged for 10 minutes at 14,000 rpm at 10°C. The supernatant was saved and the pellet discarded.

*NAD<sup>+</sup> quantification:* A two-step redox-coupled bioassay procedure was adapted from Gibon and Larher (1997).<sup>8</sup> Typical determinations of the amount of NAD<sup>+</sup> use ADH to reduce NAD<sup>+</sup> to NADH, and reading the A<sub>340nm</sub> of NADH (see Figure 4A).<sup>9</sup> However, this wavelength is shared by several other molecules that would be in the solution, contaminating the concentration value. Thus, a second part to the assay was added by Gibon and Larher, where phenazine methosulfate (PMS) uses electrons from NADH to reduce thiazoyl blue tetrazolium bromide (MTT), which is then read at A<sub>570nm</sub> (see Figure 4B).<sup>10</sup> The overall assay involved ADH (60 units/mL) utilizing NAD<sup>+</sup> as a cofactor to oxidize excess ethanol (5.0 M) to acetaldehyde in the presence of 1.0 M Tricine-KOH, pH 9.0, and 0.5 M EDTA, pH 8.0 (see Figure 4C). This reaction mix was then added to tubes consisting of different concentrations of biological samples in 0.1 M Tricine-KOH Solution, pH 9.0, and incubated for 5 minutes in a 30°C water bath. Control tubes were also concurrently run with the same assay, where commercial source NAD<sup>+</sup> (5 μM NAD<sup>+</sup> was prepared in 1.0 M Glycine/KOH buffer, pH 8.5) was used instead of the biological sample to construct a calibration curve.

A significant modification was made to the Gibon and Larher assay, for in the second step of the cycle, NADH is oxidized and converted back into NAD<sup>+</sup>, beginning the cycle anew. This, in effect, amplifies the levels of NAD<sup>+</sup> that would have been reported. Therefore, the cycle's two phases, the reduction of NAD<sup>+</sup> and the reduction of MTT, were separated by adding an irreversible inhibitor to ADH (see Figure 4D). After a 5-minute, 30°C incubation with only the reaction mixture corresponding to the first phase, the reaction was stopped with 10 mM of N-ethylmaleimide. After this step was stopped, an MTT-PMS solution was added to begin the second step of the cycle, which was incubated for 15 minutes. Results were read at A<sub>570nm</sub>.

## Results

*NAD<sup>+</sup> calibration curve:* Commercial NAD<sup>+</sup> in known concentrations was tested simultaneously using the same reaction conditions and reagents as the biological reaction (see Figure 5). A linear regression curve was fitted to the average values from eight control trials. The line representing NAD<sup>+</sup> concentration as a function of MTT absorbance is nearly linear, with the line fitting the data at an R-value of 0.991.

*NAD<sup>+</sup> concentration determination:* The average vacuolar concentration of NAD<sup>+</sup> was  $5.2 \pm 2.6$  μM, and the average NAD<sup>+</sup> concentration in the spheroplast was  $202 \pm 102$  μM (see Table 3). These estimates were based on 33 reproducible replicates of fresh and frozen vacuole and spheroplast samples. The average absorbance of these replicates was converted into moles of NAD<sup>+</sup> using the NAD<sup>+</sup> calibration curve. To determine the total moles of NAD<sup>+</sup> in a particular sample, the value from the calibration curve was divided by the volume of sample that was added to the reaction, and was then multiplied by the original volume of the biological sample solution (450 μL for vacuolar samples, 55 mL for spheroplast samples).

To determine the concentration in moles/L (M), the total concentration of NAD<sup>+</sup> in moles must be divided by the total vacuolar volume in a cell. This value was estimated by a series of steps, the first taking into account the percent yield of vacuoles or spheroplasts extracted during the isolation procedure. According to Sarry et al. (2006),<sup>3</sup> there are  $60.0 \times 10^9$  yeast cells in an

incubation mixture that has an  $OD_{600nm}$  of 1.5. As our procedure split the reaction mixture into two equivalent aliquots to assess both protein content and  $NAD^+$  content,  $30.0 \times 10^9$  yeast cells were actually assessed. According to a CPY recovery experiment found in Sarry et al. (2006),<sup>3</sup> 10.9% of CPY was retained from the spheroplast to the isolated vacuoles. As CPY is a luminal marker in the vacuole, the CPY percent recovery is the total yield of vacuoles from their spheroplasts. This measurement alone could have produced a distorted value, for CPY could have leached out, been inhibited, or been degraded by a protease. Thus, it is critical that the previously reported APE1 and  $\alpha$ -mannosidase markers co-purify with CPY, indicating the accuracy of using the CPY percent yield. CPY appears to be an appropriate standard for a recovery rate, as it is corroborated by other vacuolar markers. Thus, the estimated number of vacuoles in the sample is 10.9% of  $30.0 \times 10^9$  yeast cells, or approximately  $3.3 \times 10^9$  vacuoles in the sample. For spheroplasts, a Beckman hemacytometer was used to determine the percent yield of spheroplasts from the original number of yeast cells. This percent yield was found to be 9.6%.

To assess the total volume in the sample, the volume of one vacuole or spheroplast was determined. To determine spherical volume as  $v = (4/3)(\pi r^3)$ , the vacuolar radius of 1.5  $\mu m$  and spheroplast radius of 4.5  $\mu m$  was used, as found in Sarry et al. (2006).<sup>3</sup> These values are averages, for the radius and volume of a cellular vacuole varies widely depending on the cell's characteristics, including its phase in the cell cycle. Thus, to estimate the total volume, this volume per individual vacuole or spheroplast was multiplied by the total number of vacuoles or spheroplasts in the sample. This value was converted to liters using the conversion factor:  $1 \mu m^3 = 1 \times 10^{-15}$  L. Thus, to assess the total concentration, the number of moles of  $NAD^+$  was divided by the total volume of vacuoles or spheroplasts. After this analysis, the average concentration for  $NAD^+$  in the vacuole and spheroplast, respectively, was  $5.2 \pm 2.6 \mu M$  and  $202 \pm 102 \mu M$ . The variability was difficult to control; within a particular sample there was a degree of variation that could not be eliminated. This points to the need for additional trials to reduce the amount of deviation from the mean.

## Conclusions

Vacuolar  $NAD^+$  concentration corresponds to the  $K_m$  values for certain vacuolar dehydrogenases (Table 3). That is, the  $NAD^+$  level found in this study is on the same order of magnitude of ADH, aldehyde dehydrogenase (ALDH), and glyceraldehyde 3-phosphoglycerate dehydrogenase (G3PDH). This could mean that prevailing concentrations of vacuolar  $NAD^+$  levels may be sufficient to support at least a subset of  $NAD^+/NADH$ -coupled redox reactions. Several additional factors need to be considered, including luminal pH and presence of competitors, before asserting *in vivo* activity. However, the corresponding  $K_m$  values suggest that *in vivo* activity is a possibility inside of the vacuole.

As the steady-state vacuolar concentration of  $NAD^+$  is 0.4% of the steady-state spheroplast concentration (calculated by dividing total moles of  $NAD^+$  in each location), the vacuoles may store a potentially significant percentage of the cell's total  $NAD^+$  content. In comparison with values cited in literature, the yeast vacuole contains three orders of magnitude less  $NAD^+$  than the mitochondria and the cytoplasm as a whole (see Table 4). Further tests are needed to determine if these quantities are sufficient to be considered a storage area for  $NAD^+$ .

For instance, Hanson and Rea groups found that 10% of the folate cofactor was significant enough to be considered a store for the compound.<sup>5</sup> If  $\text{NAD}^+$  is being stored in the vacuole, further tests are needed to determine by what mechanism they are being localized there. If the vacuole is not a storage compartment for  $\text{NAD}^+$ , future inquiries should investigate the role of the  $\text{NAD}^+$  that is present in the lumen.

In light of the vacuole data, the function and role of the vacuolar dehydrogenases may need to be reconsidered. Possible explanations for the conditions under which the cofactor is being localized to the vacuole needs to be considered. Additionally, the mechanism of  $\text{NAD}^+/\text{NADH}$  traffic across the tonoplast is another avenue for investigating the role of  $\text{NAD}^+$  inside of the vacuole. Further tests also need to be conducted to identify the mode and conditions of transport of the  $\text{NAD}^+$ -dependent dehydrogenases inside of the vacuole. As the transporter for  $\text{NAD}^+$  in the mitochondria has been identified, mutant strains containing a knockout for this protein could be used to shunt  $\text{NAD}^+$  away from the mitochondria to alternate locations, possibly including the vacuole.<sup>18</sup>

In sum, if the enzymes are found to be active *in vivo*, it will open up several opportunities to expand knowledge of the role of the vacuole in a cell, and opens the possibility of reverse engineering of the dehydrogenase machinery to heighten output of compounds in processes like heavy metal detoxification. Some of these enzymes are up-regulated under cadmium stress (Table 2). The stimulation of these dehydrogenases by cadmium could be necessary to increase the flux of production of ATP, NADH, and NADPH in order to sustain the cell not only in terms of energy demand and reducing molecules, but also to synthesize carbon skeletons such as 2-oxoglutarate and phosphoglycerate, required for the synthesis of amino acids and molecules involved in cadmium chelating. Thus, there is a store of  $\text{NAD}^+$  inside of the vacuole; however, the significance of and reason for this accumulation needs further investigation.

## Acknowledgments

This work was supported by the Department of Biology at the University of Pennsylvania, and the Ronald E. McNair Post Baccalaureate Scholars Program. I thank Dr. Jean-Emmanuel Sarry, Richard Collum, and Dr. Philip A. Rea for their contributions to this work.

## References

- 1: Sanita di Toppi, L., Gabbrielli, R. *Environmental Experimental. Botany*. 1999;4:105-130.
- Chaney RL, Malik M, Li YM, Brown SL, Brewer EP, Angle JS, Baker AJ. *Current Opinion in Biotechnology*. 1997 Jun;8(3):279-284.
- 2: Yu W, Macreadie IG, Winge DR. *Journal of Inorganic Biochemistry*. 1991 Nov 15;44(3):155-161.
- 3: Sarry JE, Chen S, Collum RP, Liang S, Peng M, Lang A, Naumann B, Dzierszynski F, Yuan CX, Klionsky DJ, Hippler, M, Rea PA. Analysis of the vacuolar luminal proteome of *Saccharomyces cerevisiae*. *Journal of Biological Chemistry*, forthcoming 2006.
- 4: Suzuki KT, Sunaga H, Yamane Y, Aoki Y. *Research Communications in Chemical Pathology and Pharmacology*. 1991 Nov;74(2):223-236.
- 5: Orsomando G, de la Garza RD, Green BJ, Peng M, Rea PA, Ryan TJ, Gregory JF 3rd, Hanson AD. *Journal of Biology Chemistry*. 2005 Aug 12;280(32):28877-28884.



- 6: La Rue A, Koehler KM, Wayne SJ, Chiulli SJ, Haaland KY, Garry PJ. *The American Journal of Clinical Nutrition*. 1997 Jan;65(1):20-29.
- 7: Malouf M, Grimley EJ, Areosa SA. Folic acid with or without vitamin B12 for cognition and dementia. *Cochrane Database of Systemic Reviews*. 2003;(4):CD004514.
- 8: Gibon Y, Larher F. *Analytic Biochemistry*. 1997 Sep 5;251(2):153-157.
- 9: <http://www.r-biopharm.com>
- 10: Yim SK, Yun CH, Ahn T, Jung HC, Pan JG. *Journal of Biochemistry and Molecular Biology*. 2005 May 31;38(3):366-369.
- 11: Hou CT, Patel R, Laskin AI, Barnabe N, Barist I. *Applied and Environmental Microbiology*. 1983 Jul;46(1):178-184.
- 12: Rodriguez-Zavala JS, Ortiz-Cruz MA, Moreno-Sanchez R. *The Journal of Eukaryotic Microbiology*. 2006 Jan-Feb;53(1):36-42.
- 13: Ding Y, Ma QH. *Biochimie*. 2004 Aug;86(8):509-518.
- 14: Cioni P, Strambini GB. *Biochemistry*. 1997 Jul 15;36(28):8586-8593.
- 15: Lin SJ, Ford E, Haigis M, Liszt G, Guarente L. *Genes & Development*. 2004 Jan 1;18(1):12-16.
- 16: Theobald U, Mailinger W, Baltes M, Rizzi M, Reuss M. *Biotechnology and Bioengineering*. 1997; 55(2):305-316.
- 18: Todisco S, Agrimi G, Castegna A, Palmieri F. *Journal of Biological Chemistry*. 2006 Jan 20;281(3):1524-1531.

**Table 1. NAD<sup>+</sup>-dependent dehydrogenases<sup>3</sup>** Seven dehydrogenases were identified in *S. cerevisiae* as shown in this table. These match the proteins mapped on the 2-D gel in Figure 2. The method used for NAD<sup>+</sup> quantification exploits the major reaction catalyzed by alcohol dehydrogenase.

Gene	Protein Name	Locus	Enzymatic Reaction
ADH1	Alcohol dehydrogenase I	YOL086c	$\text{CH}_3\text{CH}_2\text{OH} + \text{NAD}^+ \rightarrow \text{CH}_3\text{CH}=\text{O} + \text{NADH} + \text{H}^+$
ADH2	Alcohol dehydrogenase II	YMR303c	$\text{CH}_3\text{CH}_2\text{OH} + \text{NAD}^+ \rightarrow \text{CH}_3\text{CH}=\text{O} + \text{NADH} + \text{H}^+$
TDH1	Glyceraldehyde 3-phosphate dehydrogenase	YJL052w	D-glyceraldehyde 3-phosphate dehydrogenase + phosphate + NAD <sup>+</sup> → 3-phospho-D-glyceroyl phosphate + NADH
TDH2	Glyceraldehyde 3-phosphate dehydrogenase	YJR009c	D-glyceraldehyde 3-phosphate dehydrogenase + phosphate + NAD <sup>+</sup> → 3-phospho-D-glyceroyl phosphate + NADH
TDH3	Glyceraldehyde 3-phosphate dehydrogenase	YGR192c	D-glyceraldehyde 3-phosphate dehydrogenase + phosphate + NAD <sup>+</sup> → 3-phospho-D-glyceroyl phosphate + NADH
ALD6	Aldehyde dehydrogenase	YPL061w	Aldehyde + NAD <sup>+</sup> + H <sub>2</sub> O → Acid + NADH
MDH2	Malate dehydrogenase	YOL126c	Malate + NAD <sup>+</sup> → oxaloacetate
LPD1	Dihydrolipoyl dehydrogenase	YFL018c	Protein N6-(dihydrolipoyl)lysine + NAD <sup>+</sup> → Protein N6-(lipoyl)lysine + NADH
GDH1	Glutamate dehydrogenase	YOR375c	L-glutamate + H <sub>2</sub> O NAD(P) <sup>+</sup> → 2-oxoglutarate + NH <sub>3</sub> + NADPH
HOM6	Homoserine dehydrogenase	YJR139c	L-homoserine + NAD(P) <sup>+</sup> → L-aspartate 4-semialdehyde + NAD(P)H

**Table 2. Activity of vacuolar markers.** Specific activity of vacuolar marker enzymes (ADH, alcohol dehydrogenase; GAPDH, glyceraldehydes 3-phosphoglycerate dehydrogenase; CPY, carboxypeptidase Y; APE1, aminopeptidase I;  $\alpha$ -mannosidase) and NAD-dependent glycolytic enzymes (GAPDH, glyceraldehydes 3-phosphoglycerate dehydrogenase; in isolated vacuoles from wild-type yeast strains after 12h-growth with or without cadmium (25  $\mu$ M, CdCl<sub>2</sub>).<sup>3</sup> Each specific activity expressed as nmol/min/mg; mean  $\pm$  SE (n=5-10 replicates). In parentheses, the ratio is the specific activity under cadmium divided by the specific activity under control conditions.

	<b>ADH</b>	<b>GAPDH</b>	<b>CPY</b>	<b>APE I</b>	<b><math>\alpha</math>- mannosidase</b>
<b>0</b>	15.9 $\pm$ 3.0	7.4 $\pm$ 1.0	36.7 $\pm$ 5.0	0.406 $\pm$	0.333 $\pm$ 0.109
<b>25</b>	20.6 $\pm$ 1.2 (130)	13.3 $\pm$ 2.2 (180)	9.6 $\pm$ 3.3 (0.26)	0.060 0.106 $\pm$ 0.017	0.243 $\pm$ 0.062 (0.73)

**Table 3. Concentration of NAD<sup>+</sup> in vacuole and spheroplast compared with select K<sub>m</sub> values of four dehydrogenases.** The order of magnitude is similar for the calculated concentration of NAD<sup>+</sup> in the vacuoles and the K<sub>m</sub> of ADH, AIDH, and G3PH. Values determined from, respectively, Hou et al. (1983),<sup>11</sup> Rodriguez-Zavala et al. (2006),<sup>12</sup> Ding et al. (2004),<sup>13</sup> and Cioni et al. (1997).<sup>14</sup>

<b>NAD<sup>+</sup></b> <b>Vacuole</b>	<b>NAD<sup>+</sup></b> <b>Spheroplast</b>	<b>ADH</b> <b>K<sub>m</sub></b> <b>(NAD<sup>+</sup>)<sup>11</sup></b>	<b>AIDH</b> <b>K<sub>m</sub></b> <b>(NAD<sup>+</sup>)<sup>12</sup></b>	<b>MDH</b> <b>K<sub>m</sub></b> <b>(NAD<sup>+</sup>)<sup>13</sup></b>	<b>GAPDH</b> <b>K<sub>m</sub></b> <b>(NAD<sup>+</sup>)<sup>14</sup></b>
μM	μM	μM	μM	mM	μM
5.2 ± 2.6	202 ± 102	8.2	5-50	2.5	19

**Table 4. Distribution of NAD<sup>+</sup> in yeast organelles.** The vacuole contains 0.4% of the NAD<sup>+</sup> in the spheroplast (by moles of NAD<sup>+</sup> in each region). The steady-state concentrations of NAD<sup>+</sup> in the whole yeast cell, the mitochondria, and the cytoplasm are all three orders of magnitude larger than that of the vacuole. Values from the whole cell were determined in Lin et al. (2004),<sup>15</sup> and the mitochondria and cytoplasm values were determined in Theobald et al. (1997).<sup>16</sup>

<b>Vacuole</b> μM	<b>Spheroplast</b> μM	<b>Whole cell<sup>15</sup></b> mM	<b>Mitochondria<sup>16</sup></b> mM	<b>Cytoplasm<sup>16</sup></b> mM
5.2 ± 2.6	202 ± 102	1.14, 1.26, 2.14	1.73	1.07

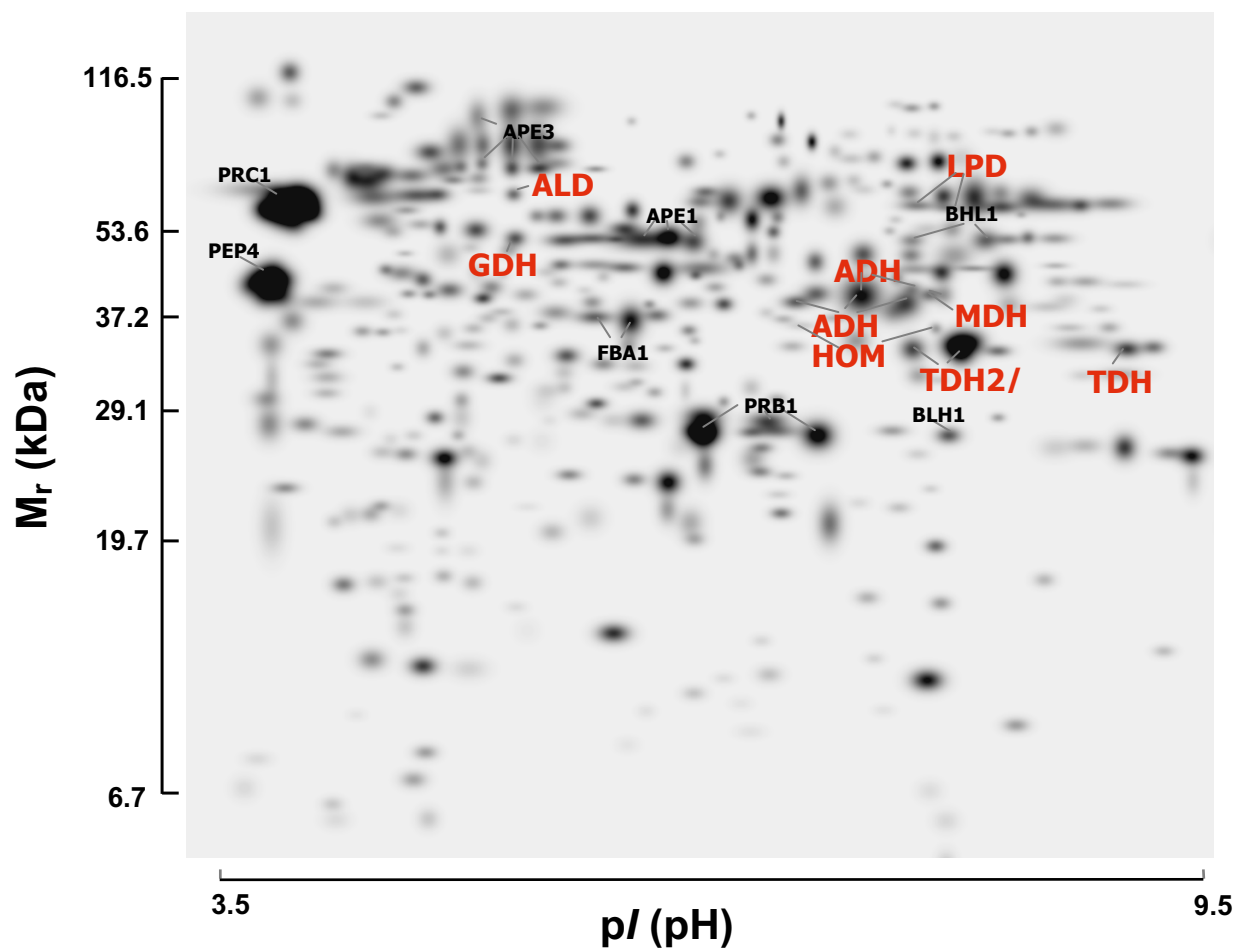


**Figure 1. Identification of vacuolar luminal proteins.** This 2-D gel electrophoresis map shows vacuolar luminal proteins from yeast, separated first by their isoelectric properties, and second by their molecular weight and identified by mass spectrometry.<sup>3</sup> Resident vacuolar proteins are labeled in black. The NAD<sup>+</sup>-dependent dehydrogenases found are labeled in red. The major reactions associated with these dehydrogenases are found in Table 1.

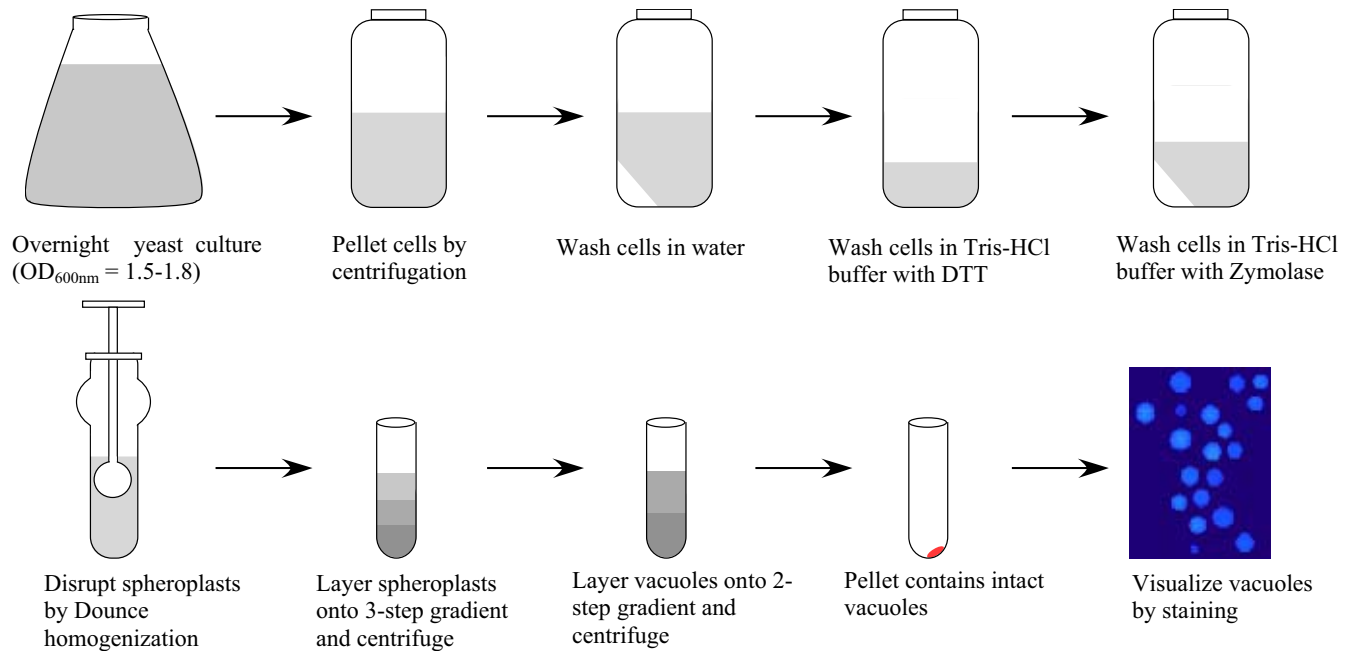


**Figure 2. Purification of yeast isolated vacuoles.** Wild-type *S. cerevisiae* colonies were incubated in an autoclaved YPD medium to an OD<sub>600nm</sub> of 1.5-1.8. Using a procedure described in Sarry et al. (2006),<sup>3</sup> the cell wall was digested away from the yeast spheroplasts using Zymolase incubation. To obtain high-purity “proteomics-grade” intact vacuoles, isolated spheroplasts were loaded onto a three-tiered gradient system involving sucrose/Ficoll buffer, and sorbitol and sucrose at differing amounts. This mixture was centrifuged, and vacuoles were collected at the sucrose/Ficoll and sorbitol:sucrose interface.

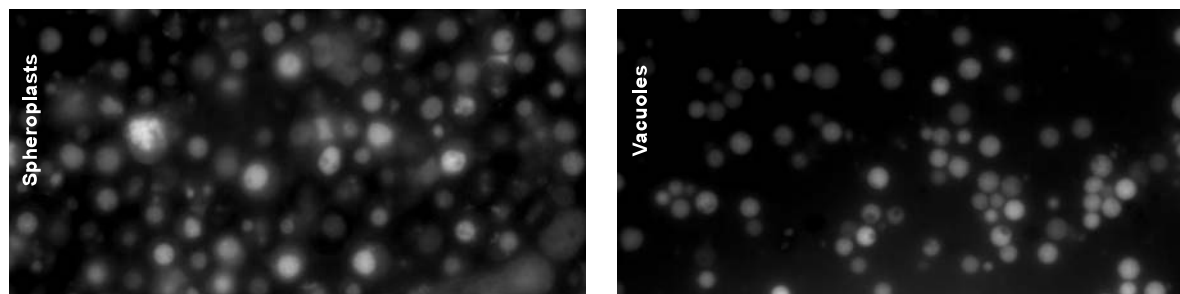


**Figure 3. Fluorescence microscopy of spheroplasts and isolated vacuoles stained with monochlorobimane (MCB).**<sup>3</sup> When in the free, unsubstituted state, MCB is membrane-permeant and non-fluorescent, but when conjugated with glutathione to yield bimane-GS it assumes a hydrophilic, membrane-impermeant, fluorescent state. Incubation and equilibration of viable yeast cells in media containing MCB thereby enables the maintenance of vacuolar integrity to be visually monitored as retention of the fluorescence is associated with bimane-GS within this compartment throughout the isolation procedure.



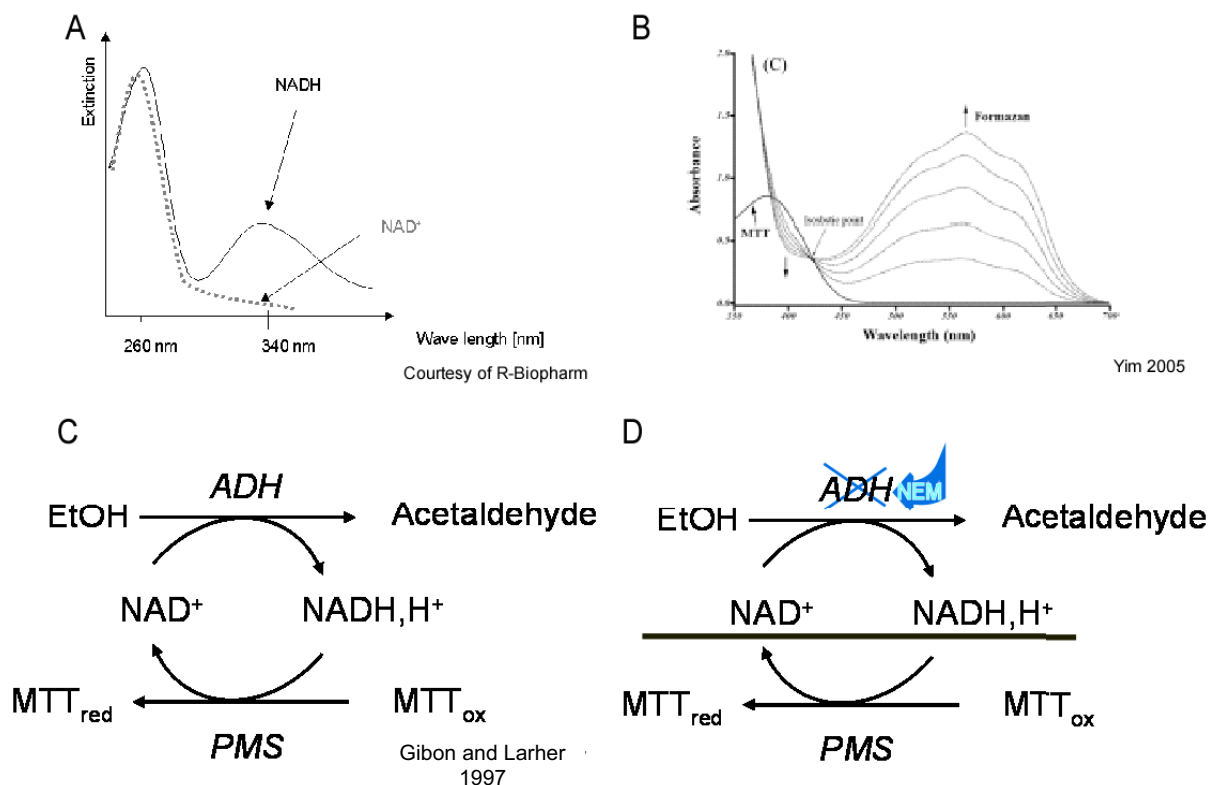


**Figure 4. Revision of two-step redox-coupled reaction assay.** A: Direct measurement of  $NAD^+$  concentration can be done by reducing it to NADH, and reading its absorbance at  $A_{340nm}$ . B: However, 340 nm is a wavelength shared by several other metabolites that would be in the same solution as our  $NAD^+$  isolation product, leading to a distortion of the absorbance of NADH alone. C: Thus, a redox-coupled assay was adopted from Gibon and Larher (1997),<sup>8</sup> where phenazine methosulfate (PMS) uses NADH to reduce thiazoyl blue tetrazolium bromide (MTT). The formazan compound is then read at  $A_{570nm}$ . This wavelength is further right on the spectrum, farther away from the UV region that many metabolites are excited at. D: The final assay involved a change in the terminal step of the cycle. In the original Gibon protocol, the reduced MTT is converted back into  $NAD^+$  and begins the cycle anew. This, in effect, amplifies the levels of  $NAD^+$  that would have been reported. Thus, the cycle's two steps, the reduction of  $NAD^+$  and the reduction of MTT, were separated by adding an irreversible inhibitor, N-ethylmaleimide (NEM), to ADH. The first step was run for 5 minutes and then stopped, and the second step began and was incubated for 15 minutes.

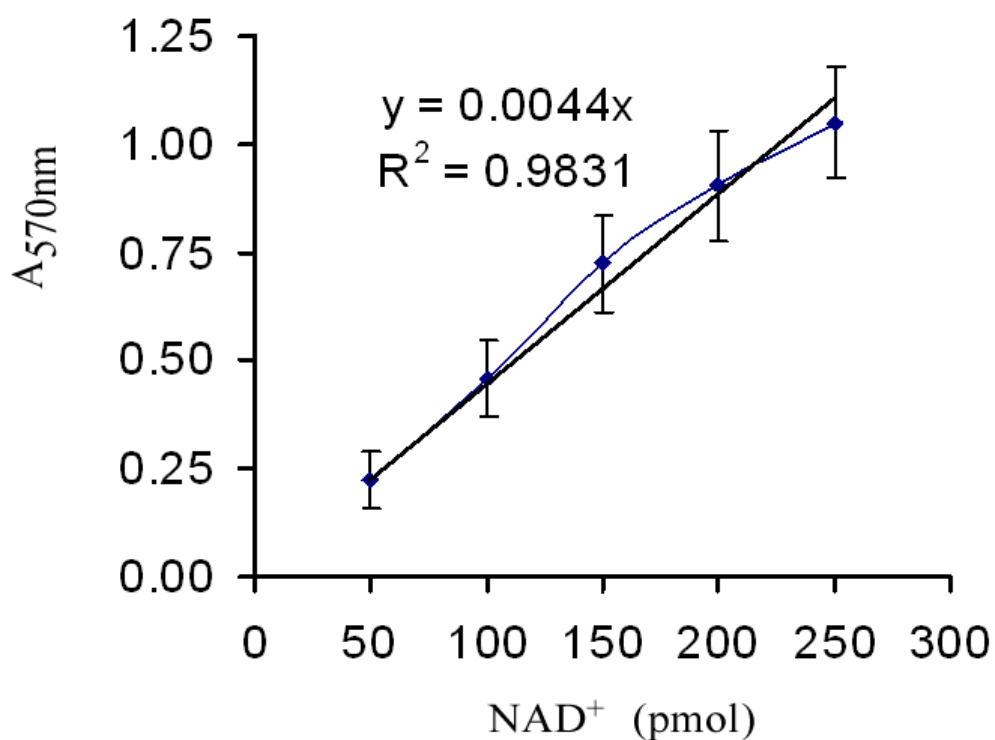


**Figure 5. NAD<sup>+</sup> calibration curve.** To determine the concentration of NAD<sup>+</sup>, a calibration curve was constructed using the absorbance of known concentrations of NAD<sup>+</sup> after incubation in the MTT coupled reaction.